Tikrit Journal of Engineering Sciences (2025); 32(4): 2193
DOI: http://doi.org/10.25130/tjes.32.4.28

IRAQI Academic Scientific Journals

ISSN: 1813-162X (Print); 2312-7589 (Online)
Tikrit Journal of Engineering Sciences
available online at: http://www.tj-es.com

TJES Tikrit Journal of Engineering Sciences

Performance of CFRP Confined Circularized Square Solid RC Columns under Bi-axial Bending (Theoretical Investigation)

Mohammed T. Jameel *

Department of Physics, College of Education, Al-Iraqia University, Baghdad, Iraq.

Keywords:
CFRP; Circularization; Solid column; Uni-axial Bending; Bi-axial Bending.

Highlights:

- *FRP confined circularized solid RC under bi-axial load.*
- *Layer-by-layer method.*
- *Number of FRP layers and concrete strength.*

ARTICLE INFO

Article history:

Received	24 May 2024
Received in revised form	20 July 2024
Accepted	24 Sep. 2024
Final Proofreading	31 Aug. 2025
Available online	26 Dec. 2025

Citation: Jameel MT. **Performance of CFRP Confined Circularized Square Solid RC Columns under Bi-axial Bending (Theoretical Investigation)**. *Tikrit Journal of Engineering Sciences* 2025; **32**(4): 2193.
http://doi.org/10.25130/tjes.32.4.28

*Corresponding author:
Mohammed T. Jameel
Department of Physics, College of Education, Al-Iraqia University, Baghdad, Iraq.

Abstract: This paper investigates theoretically the performance of square solid reinforced concrete (RC) columns circularized with concrete segments and strengthened with Carbon Fiber Reinforced Polymer (CFRP) under bi-axial load eccentricities. The layer-by-layer method is presented to calculate the axial load and bi-axial bending moment. The theoretical results were first verified with experimental results of uni-axially loaded circularized and CFRP confined square solid RC columns. Also, they were verified with experimental results of bi-axially loaded square solid RC columns that exist in the literature. It was proved that the adopted theoretical models and layer-by-layer method were in good agreement with the experimental results. After validating the reliability of the theoretical model, this study theoretically examined the performance of CFRP confined circularized square solid RC columns under bi-axial load eccentricities subjected to the effect of the number of layers of CFRP and the effect of unconfined concrete strength. It was found that circularization increased the performance of CFRP confined square solid RC columns under bi-axial eccentricity for the axial load and bi-axial moments. However, the performance was less than that of the corresponding columns subjected to uni-axial load eccentricity. Also, the performance of CFRP confinement increased with the number of CFRP layers and the unconfined concrete strength. Furthermore, the CFRP confinement performance was less significant with higher bi-axial eccentricity.

أداء الاعمدة الخرسانية المسلحة الصلدة المربعة المقطع المصنوعة من البلاستيك المقوى بألياف الكربون (CFRP) تحت الانحناء ثنائي المحور (دراسة نظرية)

محمد طارق جميل
قسم الفيزياء/ كلية التربية/ الجامعة العراقية / بغداد – العراق.

الخلاصة
الدراسة الحالية تتحرى نظريا اداء الاعمدة الخرسانية المسلحة الصلدة المربعة المقطع التي تم تغييرها الى دائرية المقطع بقطع خرسانية وحصرها بالالياف الكاربونية البوليمرية المسلحة تحت الاحمال اللامركزية المزدوجة. طريقة الطبقات استخدمت لحساب الاحمال المحورية والعزوم المزدوجة التي تقابلها. النتائج النظرية بداية تم تأكيدها مع النتائج العملية للاعمدة المربعة المسلحة الصلدة المعدلة الى دائرية والمعززة بالياف الكاربون البوليمرية المسلحة تحت تأثير الاحمال اللامركزية الاحادية الموجودة في الابحاث السابقة. ثم تم تأكيد النتائج النظرية مع الاعمدة الخرسانية المسلحة المربعة المقطع المعززة بالياف الكربون البوليمرية المسلحة تحت تأثير الاحمال اللامركزية المزدوجة. بعد تأكيد النتائج النظرية مع العملية تم دراسة اداء الاعمدة الخرسانية المسلحة الصلدة المربعة المقطع التي تم تغييرها الى دائرية المقطع وتعزيزها بالالياف الكاربونية البوليمرية المسلحة تحت الاحمال اللامركزية المزدوجة. كما تم دراسة تأثير عدد طبقات الكربون البوليمري المسلح و كذلك مقاومة انضغاط الخرسانة غير المحصورة على مخططات تداخل القوى المحورية مع العزم المزدوج للاعمدة الخرسانية المسلحة الصلدة المربعة المقطع التي تم تدويرها وتعزيزها بالالياف الكاربونية البوليمرية المسلحة. لقد تبين أن تدوير مقطع العمود يزيد اداء الاعمدة الخرسانية المسلحة الصلدة المربعة المقطع المعززة بالالياف الكاربونية البوليمرية المسلحة تحت الاحمال اللامركزية المزدوجة من حيث الاحمال المحورية والعزوم المزدوجة المقابلة لها. ولكن الاداء يكون اقل مقارنة بالاعمدة المماثلة المعرضة لاحمال لا مركزية احادية. كذلك فإن أداء الحصر بالـ(CFRP) يزداد بزيادة عدد طبقات الـ(CFRP) وبزيادة مقاومة انضغاط الخرسانة غير المعززة. واخيرا، الاداء يكون أقل اهمية مع زيادة الاحمال اللامركزية المزدوجة.

الكلمات الدالة: CFRP، التدوير، العمود الصلد، العزم الاحادي، العزم المزدوج.

1.INTRODUCTION

The change in seismic maps, the modification of structure usage, aging of structures, and degradation of structures due to the environment, in addition to the cost of demolishing and constructing new buildings, are behind the motivation of the rehabilitation of concrete structures. The strengthening of concrete structures aims to enhance the behavior of concrete in terms of strength and ductility under various applied loads. Fiber-reinforced polymer (FRP) is one of the preferred materials for strengthening and upgrading concrete members. The FRP materials are desired over steel due to their higher corrosion resistance, strength-to-weight ratio, and flexibility in strengthening concrete members against shear, bending, strength, and ductility compared to steel [1-4]. Columns are important structural members that withstand the loads from slabs and beams and transfer them to the foundation. The columns are designed according to the types of the transformed load. The types of applied loads on a specific column depend on its location. Columns can be subject to either concentric or eccentric axial loads. The eccentric loads can result in either uni-axial bending moment or bi-axial bending moment according to the position of the applied eccentric axial load with the axis of the cross-section (Fig. 1). For non-circular columns, the eccentric load in some cases applied at the same time about both principle axes, in this case the bi-axial bending design of column should be considered.

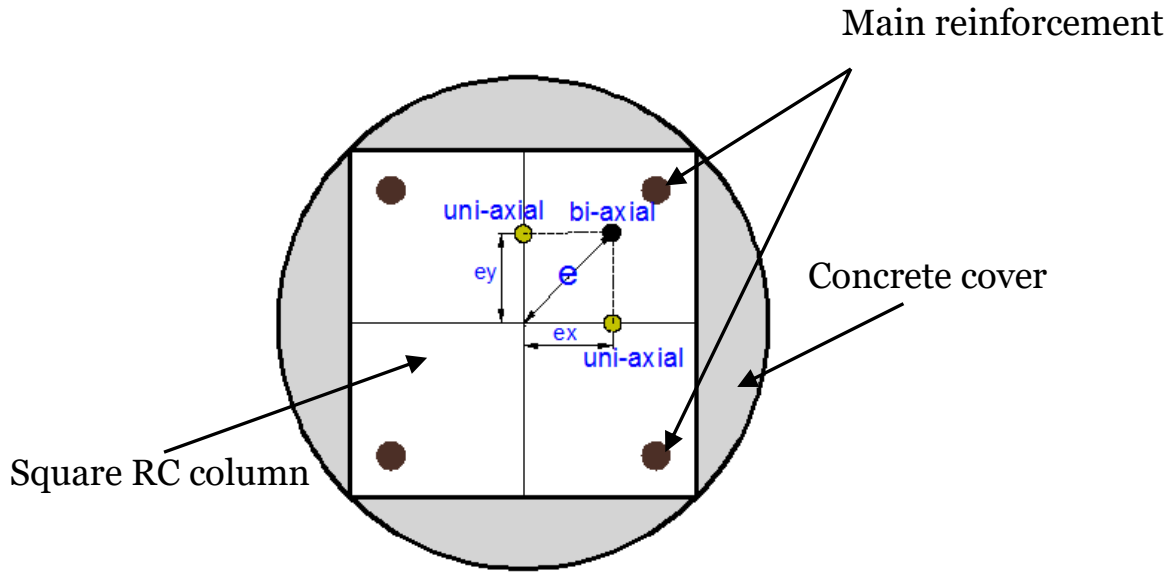

Fig. 1 Position of the Applied Eccentric Loads.

Many research studies showed that FRP confinement improves the behavior of solid concrete columns in terms of strength and ductility [5, 6]. Numerous studies investigated the confinement of columns under axial concentric loading [5-11]. Few studies have investigated the FRP confinement under uni-axial eccentric loads, in which the column is subjected to eccentric axial load and uni-axial bending moment [12-14, 15, 16]. Few research studies investigated the behavior of bi-axially loaded FRP confined solid columns [17-19]. Many research studies investigated the confinement efficiency for solid columns with a large range of corner radii [20, 21]. Most previous research studies reported that reducing the corner sharpness results in higher confinement efficiency, in which the circular sections results in the highest confinement efficiency. One of the methods to eliminate the corner sharpness is by attaching one precast concrete segment to each sides of the non-circular column. These segments change the cross-section into a circle before wrapping with the required number of FRP [22-27]. The circularization can increase the strength, ductility, and bending moment capacity of FRP confined square solid concrete columns under different uni-axial load eccentricities [22]. However, the behavior of FRP confined circularized concrete columns subjected to bi-axial bending moment is not understood. The number of transverse layers of FRP and the eccentricity of the applied load can significantly affect on the confinement. The higher number of transverse layers of FRP results in higher confinement effectiveness for solid columns as the stiffness of wrapping materials increases [8, 21, 28, 29]. Also, higher load eccentricity reduces the efficiency of confinement for solid columns. [22]. Based on the above literature, it has been found that, there was no study has examined the behavior of the FRP confined circularized square solid concrete columns subjected to bi-axial bending moment. Also, due to the square shape of the original core column of circularized specimens, bi-axial load eccentricities need to be considered. To fill this gap, this paper examines theoretically the behavior of FRP confined circularized square solid RC concrete columns subjected to bi-axial bending moment. For this purpose, constitutive confinement strength and strain models available in the literature, along with the layer-by-layer technique, are presented in this study to calculate the load and the bi-axial bending under different bi-axial eccentricities. To justify the validity of the theoretical analysis for predicting the axial load and the axial/bi-axial bending, the theoretical results were compared with the experimental results for bi-axial analysis of square solid columns [19] and uni-axial analysis of circularized solid RC columns [24]. After justifying the validity of the theoretical analysis, the axial load-bi-axial bending moment interactions are presented, and a parametric study was conducted to investigate the effects of the number of CFRP layers, as well as different unconfined concrete strengths, on the axial load and corresponding bi-axial bending moment. The methodology of the analysis is deeply detailed in the theoretical section.

2.THEORETICAL ANALYSIS

In this section, theoretical analysis for the FRP confined solid RC column's section is presented to calculate the axial load-uni-axial/bi-axial bending moment for columns under load eccentricities. The assumptions of the section analysis before and after the analysis are explained. The constitutive strength and strain models for unconfined and confined concrete available in the literature are adopted to determine the ultimate confinement strength and strain, in addition to stress-strain formulas. Also, the modeling of steel bars and FRP sheets is detailed. The analysis process and steps for the layer-by-layer method, in which the section is divided into layers, are illustrated.

2.1.Modelling of Circularized Solid Concrete Specimens Confined with FRP

The literature showed that the behavior of circularized specimens is similar to that of circular specimens [22, 24]. Therefore, the circularized specimens in this study are modeled as circular specimens regardless of the probable debonding between the precast concrete and the core column. The lateral expansion of concrete due to Poisson's effect results in the confinement of the wrapped FRP, which resists the increased diameter and changes the state of stresses of concrete from bi-axial into tri-axial. Based on the equilibrium of the forces on the confined section, the FRP confinement pressure ($f_{conf.}$) is determined as:

$$\mathbf{f_{conf.}} = \frac{\mathbf{2(E_{frup} k_{\varepsilon}\, \varepsilon_{frp})t}}{\mathbf{2R}}\ \mathbf{(MPa)} \qquad \mathbf{(1)}$$

where E_{frup} is the elastic modulus of FRP, t is the nominal thickness of FRP, R is the radius of the column, and k_{ε} is the strain efficiency factor; a value of 0.586 was used for k_{ε}, which was initially used in Lam and Teng [30] and multiplied by the ε_{frp}, i.e., the maximum FRP strain in the coupon test, to present the real rupture strain of FRP (ε_{frup}).

Lam and Teng [30] presented a model to determine the strength for circular concrete columns confined with FRP, as follows:

$$\frac{\mathbf{f_{cc}^{'}}}{\mathbf{f_{co}^{'}}} = \mathbf{1 + k}\ \frac{\mathbf{f_{conf.}}}{\mathbf{f_{co}^{'}}} \qquad \mathbf{(2)}$$

where $f_{co}^{'}$ is the unconfined concrete strength, $f_{cc}^{'}$ is the compressive strength of FRP confined concrete, and k is a factor used, i.e., equals 3.3.

In the present study, the strain at ultimate stress of FRP confined concrete developed in Lam and Teng [31] was used as:

$$\varepsilon_{cu} = \varepsilon_{co}\left[1.75 + 12\,\frac{f_{conf.}}{f'_{co}}\left(\frac{\varepsilon_{h,rup}}{\varepsilon_{co}}\right)^{0.45}\right] \quad (3)$$

where $\frac{\varepsilon_{h,rup}}{\varepsilon_{co}}$ represents the FRP hoop rupture strain divided by the unconfined axial strain corresponding to the unconfined concrete strength f'_{co}, and ε_{cu} is the strain at ultimate stress of FRP confined concrete.

The stress at a certain strain of confined concrete specimens was calculated by adopting the Lam and Teng's model [31], as follows:

$$f'_{ci} = \begin{cases} E_c\varepsilon_c - \frac{((E_c - E_2))^2}{4f'_{co}}\varepsilon_c^2 \text{ for } 0 \le \varepsilon_c \le \frac{2f'_{co}}{E_c - E_2} & (4) \\ f'_{co} + E_2\varepsilon_c \text{ for } \varepsilon_t \le \varepsilon_c \le \varepsilon_{cu} & (5) \end{cases}$$

where $\frac{2f'_{co}}{E_c - E_2}$ is the portion of transition between the linear first stage (unconfined concrete) and the second stage (confined concrete) in the axial stress-axial strain behaviour, ε_c is the axial strain corresponding to stress (f_c) of the confined concrete, ε_{cu} is the ultimate compressive strength of the confined concrete, $\frac{f'_{cc} - f'_{co}}{\varepsilon_{cu}}$ is the slope of linear second part of the axial stress- axial strain curve of confined concrete, and E_c is the modulus of elasticity (the slope of the first part). E_c was calculated according to ACI 318 M-2011 [32], as follows:

$$E_c = 4730\sqrt{f'_{co}} \quad (\text{MPa}) \quad (6)$$

2.2.Modeling of RC Columns

The confinement of steel ties was ignored in this paper, according to ACI 318 M-2011 [32], similar to that of circular steel helices. The compressive strength of the unconfined concrete was calculated by the axial stress-axial strain model proposed in Popovics [33], as follows:

$$f_c = f'_{co}\,\frac{\upsilon\,\varepsilon_c}{\varepsilon_{co}\,(\upsilon - 1 + (\frac{\varepsilon_c}{\varepsilon_{co}})^{\upsilon})} \quad (7)$$

$$\upsilon = \frac{E_c}{E_c - \frac{f'_{co}}{\varepsilon_{co}}} \quad (8)$$

The model developed by Tasdemir et al. [34] was adopted to determine ε_{co} according to:

$$\varepsilon_{co} = \left(-0.0067\,f'^{\,2}_{co} + 29.9\,f'_{co} + 1053\right) \times 10^{-6} \quad (9)$$

2.3.Steel Reinforcement Modelling

It is well known that the behavior of steel used as reinforcement is elastic up to the yield strength (f_{sy}). The axial compressive stress and axial tensile stress of steel bars (f_s) were calculated by multiplying the axial strain (ε_s) by the elastic modulus (E_s), to yield:

$$f_s = E_s\,\varepsilon_s \le f_{sy} \quad (10)$$

2.4.Modeling of FRP Materials

The FRP is a linear elastic material, in which the tensile stress of FRP was calculated as:

$$f_{Frp} = E_{Frp}\,\varepsilon_{Frp} \le f_{frup} \quad (11)$$

2.5.Axial Load-Bending Moment Interactions (Theoretical Modelling using Layer by Layer Method)

In this study, the layer-by-layer method was presented to determine the axial load-bending moment behavior where, the column's section was divided into a finite number of layers with Δh thickness (Δh = 1mm in this study). Only the compressive strength of concrete was considered, while the concrete was neglected in the tension zone. The plain section was assumed to remain plain under bending and the slip between the concrete and the embedded steel reinforcement and/or the FRP was neglected. Also, no debonding was assumed between the concrete segments and the square column. Figure 2 illustrates the sketch of the cross-section for the circularized specimens. The details of the symbols in Fig. 2 are as follows:

$$y_i = R_o - \Delta h(i - 0.5) \quad (12)$$

where y_i is the distance between the center of the i_{th} layer and the center of the circular section, R_o is the radius of the circular section, and i is the distance between the furthest top point of the section and the bottom of the i_{th} layer (Fig. 2).

where the width of the i_{th} layer was calculated as:

$$b_{li} = 2\sqrt{(R_o^2 - y_i^2)} \quad (13)$$

The axial strain at the center of the i_{th} layer (ε_{ci}) is a linear promotional ($\frac{y_i}{d_N}$) to the maximum axial strain at the furthest compressed fibre (ε_{cu}), along the depth of the cross-section, as shown in Fig. 2, and was calculated as:

$$\varepsilon_{ci} = \varepsilon_{cu}\,\frac{y_i}{d_N} \quad (14)$$

where d_N is the distance from the furthest compression fibre to the neutral-axis.

The stress at the i_{th} layer (f'_{ci}) was calculated using the stress-strain model developed by Lam and Teng [31] for FRP confined concrete (Eqs. 9 and 10).

After determining the stress and strain at each layer, the axial load of the i_{th} layer was determined as:

$$P_{ci} = f'_{ci}\,A_{ci} \quad (15)$$

where (A_{ci}) is the area of the i_{th} layer.

The bending moment(M_{ci}) in the i_{th} layer was calculated as follows:

$$M_{ci} = P_{ci}\,y_i \quad (16)$$

where (P_{ci}) is the load in the i_{th} layer.

The strain at each longitudinal steel bar (ε_{si}) was calculated from:

$$\varepsilon_{si} = \varepsilon_{cu}\,\frac{d_N - d_{si}}{d_N} \quad (17)$$

where d_{si} is the distance between the centre of the steel bar and the centre of the circular section. The negative and positive values of ε_{si} refer to the condition of the longitudinal steel

bar under tension and compression, respectively.

The compressive and tensile stresses (f_{si}) of the longitudinal steel bar were calculated by multiplying the elastic modulus of the steel bar (E_s) by the strain of the steel bar (ε_{si}) as:

$$f_{si} = E_s \varepsilon_{si} \leq f_{sy} \quad (18)$$

where f_{sy} is the yield stress of the steel bar.

The tensile force/compressive force (F_{si}) of the longitudinal steel bar was determined by the multiplication of the tensile/compressive stress (f_{si}) by the area of the steel bar (A_{si}), as follows:

$$F_{si} = A_{si} f_{si} \quad (19)$$

The total axial load of the specimens was determined from:

$$P_u = 0.85 \sum_{i=1}^{n} P_{ci} + \sum_{i=1}^{ns} F_{si} \quad (20)$$

The total moment of the specimens was determined from:

$$M_u = \sum_{i=1}^{nl} M_{ci} + \sum_{i=1}^{nsb} F_{si} y_{si} \quad (21)$$

where nl is the layers' number of concrete in the circular section, and nsb is the number of longitudinal steel bars. The eccentricity was calculated by dividing M_u by P_u. The theoretical calculations were applied using an Excel sheet. An initial value of eccentricity (e) was used. Then, by iterations, the calculations continued until the required eccentricity was reached. Then, the iterations stop, in which the values of axial load and bending moment were adopted.

In this section, the available experimental results were adopted to justify the aforementioned theoretical analysis, in predicting the axial load-uni-axial/bi-axial bending moment for the CFRP confined circularized solid RC columns. The theoretical results were justified with the experimental results in Punurai et al. [19] for bi-axial analysis of square solid RC columns and with the experimental results in Pham et al. [24] for uni-axial analysis of circularized solid RC columns. Details of the experimental investigations and results, including failure mode, axial load-axial deformation behaviors, and flexural behavior, were reported in Punurai et al. [19] and Pham et al. [24]. The experimental program for each study was briefly detailed.

3.1.Experimental Study in Punurai et al. [19]

Punurai et al. [19] tested five CFRP-wrapped RC slender columns under combined axial load-bi-axial bending moment, i.e., tested to failure. The specimens were designed with a quarter scale. The specimens were designed according to the ACI code with a square cross-section of 76mm side length and 1220mm length. The bi-axial eccentric loading of 50.8mm was applied by heavy RC loading brackets of 178x178x203 mm cast at each side. The compressive strength of concrete was targeted to be 40MPa. The steel reinforcement of the specimens was designed with four No.10 rebars as main longitudinal reinforcement tied with gage 12 plain steel as transverse reinforcement distributed at 76mm center-to-center space. The concrete cover was 12.7mm. The first specimen was designed as a control specimen without CFRP wrapping. Four specimens were confined with CFRP sheets. The CFRP sheets were applied as follows: One transverse CFRP layer, double transverse CFRP layers, one longitudinal layer, and a combined longitudinal layer and transverse layer for the second, third, fourth, and fifth specimens, respectively. However, only the specimen that was wrapped with two transverse layers of CFRP was considered in the present study. All specimens were subjected to displacement-controlled loading of 1.3mm increments per minute. The strength, ductility, and failure mode were reported. More details are reported in [19].

3.2.Experimental Study in Pham et al. [24]

Pham et al. [24] investigated experimentally the behavior of CFRP-wrapped square solid concrete columns circularized with precast concrete segments having different compressive strengths. Sixteen reinforced concrete columns were prepared and tested. The columns were classified into four groups of four columns. The columns in the first group were circularized with concrete segments having the same concrete strength as the core solid column, and then confined with three CFRP layers. The square cross-section of columns in the second and third groups was changed to circular using concrete segments having the concrete strength of 43MPa and 100MPa, respectively, and then wrapped with three layers of CFRP. However, only the columns in the first group were considered for verification in the present study. The core specimens were designed with a square cross-section of 150mm side length and 800mm height, and the circularized specimens had a 212.12mm diameter. The steel reinforcement of all specimens was four 12 mm deformed longitudinal bars of 568MPa tensile strength and 6mm plain transverse steel ties of 478MPa tensile strength placed at 120 mm center to center. The compressive strength of concrete was 44MPa. Three specimens from each group were tested as columns under axial concentric, 25 mm axial eccentric and, 50 mm axial eccentric loads. One specimen from each group was tested as beam under a four-point load. The average maximum tensile force per unit length of the wrapping material (CFRP) from the coupon test performed according to ASTM D7565 [35] was 2089N/mm, the strain at the maximum tensile strength was 0.0174mm/mm, and the modulus of elasticity was 121kN/mm. More details of the experimental study can be found in Pham et al. [24].

3.3.Verification of Theoretical Axial Load-Bi-axial Moment Interactions for Square Solid RC Specimens with the Experimental Results

Table 1 shows the experimental results of the research studies selected from the literature versus the theoretically calculated results. The experimental moment of the tested column specimens and beam specimens was calculated from Eqs. 22 and 23.

$$M_u = P_{max}\,(e + \delta) \quad \textbf{(22)}$$

$$M_u = P_{max}\,(l/6) \quad \textbf{(23)}$$

where P_{max} is the maximum axial load, e is the applied eccentricity, δ is the lateral deflection, and l is the length of the span for the beam specimens, i.e., $l = 700$ mm for the FRP confined circularized beam specimen. For the FRP confined square solid RC columns subjected to bi-axial bending moments, the experimental axial loads were 1.04 and 1.02 times the theoretical axial load for specimens C2 and C4, respectively. Also, the experimental bi-axial bending moment was 1.04 percent and 1.03 times the theoretical bi-axial bending moment for specimens C2 and C4, respectively. For the FRP confined circularized square RC columns subjected to uni-axial bending moments, the experimental axial loads were 0.99, 0.86, and 0.87 times the theoretical axial load for specimens in group Cf under concentric load, 25 mm eccentric, load and 50 mm eccentric load, respectively. Also, the experimental uni-axial bending moment was 1.1 and 0.96 times the theoretical uni-axial bending moment for specimens in group Cf under 25 mm eccentric load and 50 mm eccentric load, respectively. It is clear from Table 1 that the layer-by-layer technique with the aforementioned confined and unconfined concrete models was in good agreement with the experimental results.

3.4.Theoretical Axial Load-Bi-axial Bending Moment Interactions for Circularized CFRP Confined Solid Square RC Specimens (Parametric Study)

The axial load-bi-axial bending was compared with its counterpart's axial load-uni-axial bending moment to investigate the effect of loading conditions. Furthermore, to evaluate the influence of the number of CFRP layers and the influence of different concrete compressive strength on the behavior of circularized square solid RC specimens, a parametric study was conducted theoretically.

The specimens considered were a square solid RC specimen of 150 mm side length and 800mm height that was modified into a circular section of 212mm diameter and confined with a different number of CFRP layers. The steel reinforcement of core square RC specimen was four deformed bars of 500MPa tensile strength and 12mm diameter as main reinforcement tied with plain steel of 250MPa and 6mm diameter as stirrups. The CFRP had a 500MPa tensile strength per unit length and 0.016mm/mm ultimate tensile strain. Both the core square RC specimen and the circularizing concrete segments were considered with 47MPa concrete strength. The aforementioned models and the layer-by-layer method were utilized to present the axial load-bending moment interactions. The considered circularized RC columns are classified into two groups. The specimens in the first group were subjected to concentric, 25mm uni-axial load eccentricity, 50mm uni-axial load eccentricity, and four-point load. The specimens in the second group were subjected to concentric, 25mm bi-axial load eccentricity, 50mm bi-axial load eccentricity, and four-point load. The considered specimens are nominated as follows: the C letter refers to Circularized, the F letter refers to FRP wrapping, and then the B or U refers to either Bi-axial or Uni-axial load eccentricity. The n, i.e., 1,2, 3, or 4, refers to the number of CFRP layers, and the f'c, i.e., 30,35, 40, or 45, refers to the compressive strength of unconfined concrete. For example, CFB-n=3 refers to the specimen circularized and wrapped with three layers of CFRP and subjected to bi-axial load eccentricity, and specimen CFU-f'c=35 refers to the specimen circularized and wrapped with CFRP having concrete of 35MPa unconfined compressive strength.

Table 1 Experimental vs. Theoretical Results.

Study	Specimen as nominated in the experimental study	Load Eccentricity		Load (P) (kN)			Bending moment (M) (kN-m)		
		ex (mm)	ey (mm)	Exp.	Theo.	P_{Exp}/P_{Theo}	E_{Exp}	$T_{Theo.}$	$M_{Exp}/M_{Theo.}$
Punurai et al. [19]	C2	50.8	50.8	43.6	41.8	1.04	3.13	3	1.04
	C4	50.8	50.8	45	44	1.02	3.23	3.14	1.03
Pham et al. [24]	Cf-0	0	0	3400	3411	0.99	-	-	-
	Cf-25	25	0	1513	1756	0.86	49	44	1.1
	Cf-50	50	0	969	1117	0.87	53.5	56	0.96
	Cf-f	flexural	0	0	0	0	43	20.8	-

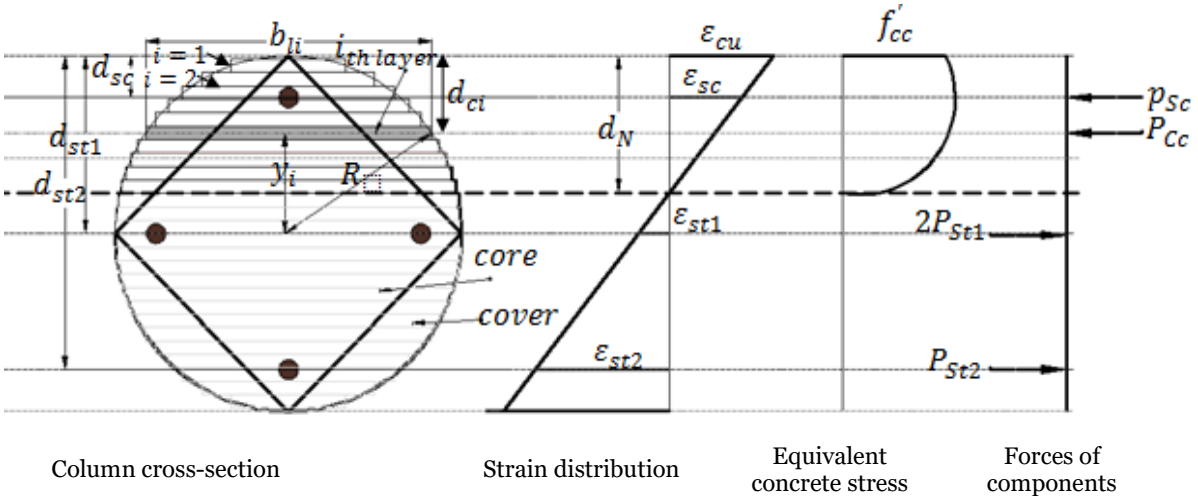

Fig. 2 Sketch of Stress and Strain Profile of FRP Confined Circularized Column under bi-Axial Load Eccentricity with (Layer by Layer Method).

3.4.1.Effect of Number of Layers of CFRP on The Axial Load-Uni-axial Bending Moment and Axial Load-Bi-axial Bending Moment Interactions for Circularized Square Solid RC Columns (Comparative Study)

Two groups were considered to examine the influence of the number of CFRP layers (1, 2, 3, and 4) on the axial load and corresponding bending moment of the CFRP confined circularized columns. Figure 3 presents the axial load-bi-axial bending interactions for the RC columns circularized and wrapped with different numbers of layers of CFRP (nL=1, 2, 3, and 4). Figure 3 shows that the ultimate axial load and the corresponding bi-axial bending of the circularized RC columns increased with the number of CFRP layers under bi-axial load eccentricity. However, the effectiveness of CFRP number of layers on the axial load and bi-axial bending moment decreased with the increased load eccentricity. Similar outcomes were reported by Li and Hadi [36]. This behavior can be explained by the reduced compression zone of the concrete section, and the column becomes more controlled by the tension failure with the increased eccentricity.

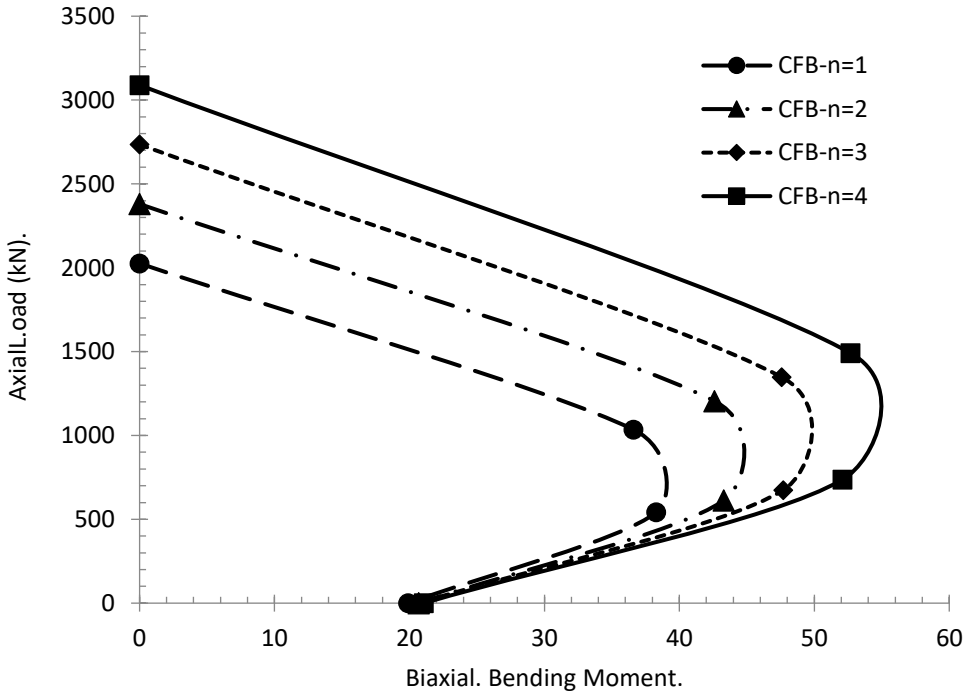

Fig. 3 Axial Load-bi-Axial Bending Moment Diagram of Circularized Columns Wrapped with Different Numbers of CFRP Layers.

Figure 4 presents the comparative behavior between the uni-axially and bi-axially loaded circularized square solid RC columns with different numbers of CFRP layers (1, 2,3, and 4). It can be clearly seen in Fig. 4 that the CFRP performance was lower for bi-axially loaded specimens than their counterparts, uni-axially loaded specimens with the same number of CFRP layers. The difference in the axial load was high for the columns when subjected to 25mm eccentricity compared to 50mm eccentricity. Also, the uni-axially loaded specimens under 25mm load eccentricity showed higher bending moment than their counterpart bi-axially loaded specimens for different numbers of CFRP layers. However, it is clear from Fig. 4 that the higher moment for uni-axially loaded specimens than the bi-axially loaded specimens was more significant when the specimens were subjected to 25mm eccentricities than that of 50mm eccentricities. This behavior is due to the arrangement of the steel geometry in both cases. The two main steel bars were under compression, and the other two steel bars were under tension for the uni-axially loaded specimen. While for the bi-axially loaded specimens, there was one steel bar in the compression region and another steel bar in the tension region. On the other hand, for specimens subjected to 50mm load eccentricity, most of the steel bars became under tension position for uni-axially and bi-axially loaded specimens, which can reduce the difference between the two cases.

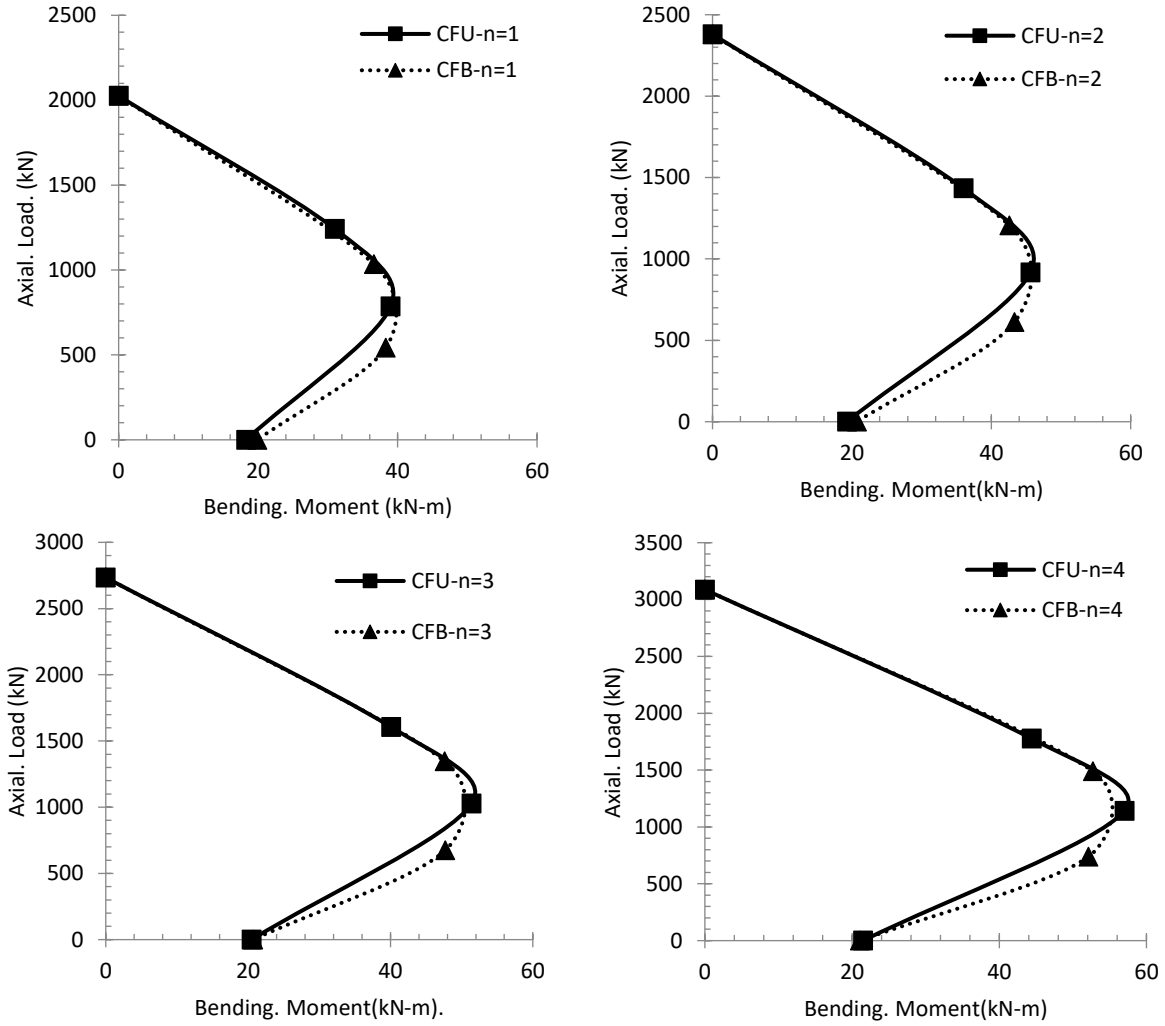

Fig. 4 Comparative Axial Load-Bending Moment Diagram of Uni-Axially and Bi-Axially Loaded Circularized Columns Wrapped with Different Numbers of CFRP Layers.

3.4.2.Effect of Unconfined Concrete Compressive Strength on the Axial Load-Uni-axial Bending Moment and Axial Load-Bi-axial Bending Moment Interactions for Circularized Square Solid RC Columns (Comparative Study)

To examine the effect of unconfined concrete compressive strength on the axial load-bending moment interaction of bi-axially loaded CFRP confined circularized concrete columns and compare the results with their counterparts, uni-axially loaded specimens, two groups of four specimens were considered herein. Specimens in the first group were subjected to bi-axial load eccentricity, while the specimens in the second group were subjected to uni-axial load eccentricity. The four specimens in each group were considered to have different

unconfined concrete compressive strengths of 30, 35, 40, and 45. Figure 5 presents the axial load-bi-axial bending moment interactions for the circularized RC specimens. Figure 5 shows that the ultimate axial load and the corresponding bi-axial bending moment of the circularized RC columns increased with the unconfined concrete compressive strength under bi-axial load eccentricity. However, the effectiveness of the unconfined concrete compressive strength on the axial load and corresponding bi-axial bending moment decreased with the increase in the load eccentricity. This behavior can be due to the reduction in the compression zone of the concrete section, in which the confined concrete is reduced with the increased eccentricity.

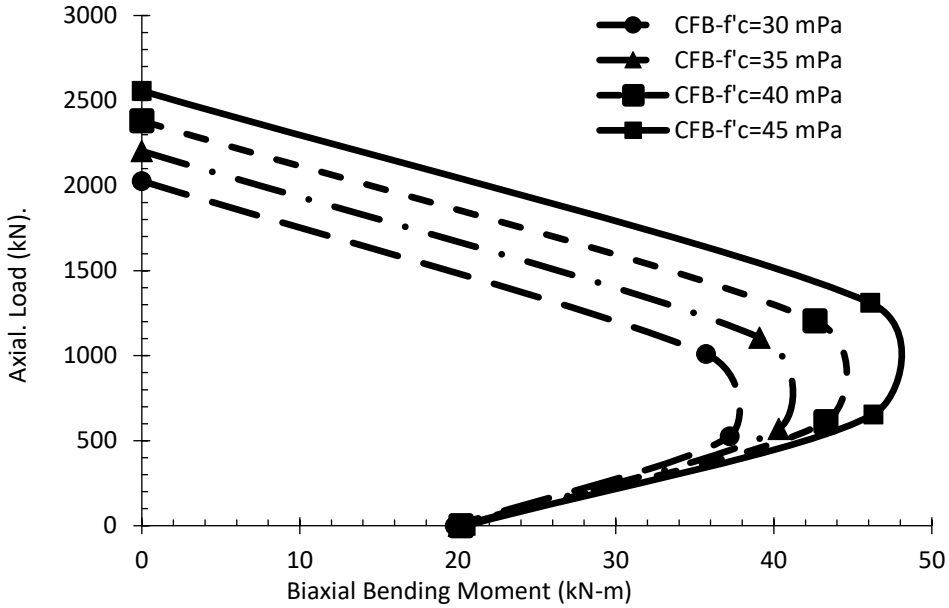

Fig. 5 Axial Load-bi-Axial Bending Moment Diagram of Circularized Columns Wrapped with Different Unconfined Compressive Strengths of Concrete.

Figure 6 compares the uni-axially and bi-axially loaded circularized square solid RC columns with different unconfined concrete compressive strengths of 30, 35, 40, and 45 MPa. It can be clearly seen in Fig. 6 that the CFRP performance was lower for bi-axially loaded specimens than their counterparts, uni-axially loaded specimens with the same unconfined concrete compressive strength. The difference in the axial load was high for the columns when subjected to 25mm eccentricity compared to 50mm eccentricity. Also, the uni-axially loaded specimens under 25mm load eccentricity showed higher bending moment than their counterpart bi-axially loaded specimens for unconfined concrete compressive strength. However, it is clear from Fig. 6 that the higher moment for uni-axially loaded specimens than the bi-axially loaded specimens was more significant when the specimens were subjected to 25mm eccentricities than that of 50mm eccentricities. This result might be because of the arrangement of the steel geometry in both cases. The two main steel bars were under compression, and the other two steel bars were under tension for the uni-axially loaded specimen. For the bi-axially loaded specimens, one steel bar was in the compression region, and one steel bar was in the tension region. On the other hand, for specimens subjected to 50mm load eccentricity, most of the steel bars became under tension position for uni-axially and bi-axially loaded specimens, which can reduce the difference between the two cases.

4.CONCLUSIONS

This study investigates theoretically the axial load-bi-axial bending moment of the circularized and CFRP confined RC columns. The theoretical study was justified with previous experimental studies. Then, it investigated the effect of the number of CFRP layers and the unconfined concrete compressive strength on the axial load-bi-axial bending moment of the square circularized and CFRP confined RC specimens under different uni-axial and bi-axial load eccentricities. According to the theoretical results, the following conclusions are drawn:

- The layer-by-layer method with Lam and Teng's models showed reasonable theoretical results for the axial load and bi-axial bending moment compared to the experimental results adopted from the literature.
- The increased number of layers of CFRP increased the performance of the axial load and bi-axial bending moment of the circularized CFRP confined concrete specimens. However, the performance decreased with the increased load eccentricity. It was the highest for the concentrically loaded specimens..

- The increased unconfined concrete compressive strength increased the performance of the axial load and bi-axial bending moment of the circularized CFRP confined concrete specimens. However, the performance decreased with the increased load eccentricity. It was the highest for the concentrically loaded specimens.
- The CFRP confined circularized concrete specimens sustained lower axial load and bending moment when subjected to bi-axial load eccentricity compared to uni-axial load eccentricity.

ACKNOWLEDGEMENTS

The author is grateful for the support towards this research by Al-Iraqia University/ College of Education. The title of this paper was approved by the College of Education at its first council session in 2023-2024, held on 10/09/2023.

NOMENCLATURE

RC	Reinforced Concrete
$CFRP$	Confinement with Fiber Reinforced Concrete
E_{frup}	Elastic Modulus of FRP, GPa
t	Nominal Thickness of FRP, mm
R	Radius of the Column, mm
f'_{co}	Unconfined Concrete Strength, MPa
f'_{cc}	Compressive Strength of FRP Confined Concrete, MPa
E_c	Modulus of Elasticity of Unconfined, GPa
E_2	Modulus Of Elasticity of Confined Concrete, GPa
E_s	Elastic Modulus of Steel, GPa
E_{Frp}	Elastic Modulus of FRP, GPa
y_i	Distance from the Furthest Compression Fiber to the Neutral-Axis, mm
R_o	Radius of the Cross Section, mm
b_{li}	Number of Layer
d_N	Distance from the Furthest Compression Fiber to the Neutral-Axis, mm
P_{ci}	Axial Load of the i_{th} Layer, N
M_{ci}	Bending Moment(M_{ci}) in the i_{th} Layer, N-m
P_u	Axial Compressive Load of the Specimens, N
M_u	Moment Capacity of the Specimens, N-m
P_{max}	Maximum Axial Load, N
e	Applied Eccentricity, mm
ex	Eccentricity in the X axis, mm
ey	Eccentricity in the y axis, mm
Greek symbols	
$f_{conf.}$	Confinement Pressure of FRP, MPa
k_ε	Strain Efficiency Factor
ε_{frup}	Maximum Strain of FRP mm/mm
$\varepsilon_{h,rup}$	Hoop Rupture Strain of FRP, mm/mm
ε_{co}	Axial Strain of Unconfined Concrete, mm/mm
ε_{cu}	Strain at Ultimate Stress of FRP Confined Concrete, mm/mm
f_s	Axial Compressive Stress and Axial Tensile Stress of Steel, MPa
f_{sy}	Yield Strength of Steel, MPa
ε_s	Axial Strain of Steel, mm/mm
f_{Frp}	Axial Tensile Stress of FRP, MPa
ε_{Frp}	Axial Strain of FRP, mm/mm
ε_{ci}	Axial Strain At the Centre Of The i_{th} Layer, mm/mm
δ	Lateral Deflection, mm

REFERENCES

[1] Abdulla AI. **Behavior of RC Beams Strengthened by CFRP and Steel Rope under Frequent Impact Load**. *Journal of Advanced Sciences and Engineering Technologies* 2018; **1**(1): 30-42.

[2] Abdulla AI, Mahasneh KN, Shaheen MW, Khazaal AS, Ali MI. **Behavior of Reinforced Concrete Beams Strengthened by CFRP and Wire Rope**. *Journal of Advanced Sciences and Engineering Technologies* 2018; **1**(3): 33-45.

[3] Al-Hazragi A-a-SI, Lateef AM. **Behaviour of Uniaxial Reinforced Concrete Columns Strengthened with Ultra-High Performance Concrete and Fiber Reinforced Polymers**. *Tikrit Journal of Engineering Sciences* 2021; **28**(2): 1-13.

[4] Hardan SA, Aules WA. **Analysis of CFRP Confined Concrete Cylinders by Using Abaqus Software**. *Tikrit Journal of Engineering Sciences* 2022; **29**(2): 28-40.

[5] Rochette P, Labossiere P. **Axial Testing of Rectangular Column Models Confined with Composites**. *Journal of Composites for Construction* 2000; **4**(3): 129-136.

[6] Silva MAG. **Behavior of Square and Circular Columns Strengthened with Aramidic or Carbon Fibers**. *Construction and Building Materials* 2011; **25**(8): 3222-3228.

[7] Razvi S, Saatcioglu M. **Confinement Model for High-Strength Concrete**. *Journal of Structural Engineering* 1999; **125**(3): 281-289.

[8] Parvin A, Jamwal AS. **Performance of Externally FRP Reinforced Columns for Changes in Angle and Thickness of the Wrap and Concrete Strength**. *Composite Structures* 2006; **73**(4): 451-457.

[9] Mirmiran A, Shahawy M. **Behavior of Concrete Columns Confined by Fiber Composites**. *Journal of Structural Engineering* 1997; **123**(5): 583-590.

[10] Matthys S, Toutanji H, Audenaert K, Taerwe L. **Axial Load Behavior of Large-Scale Columns Confined with Fiber-Reinforced Polymer Composites**. *ACI Structural Journal* 2005; **102**(2): 258-267.

[11] Faustino P, Chastre C, Paula R. **Design Model for Square RC Columns under Compression Confined with CFRP**. *Composites Part B: Engineering* 2014; **57**: 187-198.

[12] Hadi MNS. **The Behaviour of FRP Wrapped HSC Columns under Different Eccentric Loads**. *Composite Structures* 2007; **78**(4): 560-566.

[13] Hadi MNS. **Behaviour of FRP Strengthened Concrete Columns**

under Eccentric Compression Loading. *Composite Structures* 2007; **77**(1): 92-96.

[14] Hadi MNS. **Behaviour of FRP Wrapped Normal Strength Concrete Columns under Eccentric Loading**. *Composite Structures* 2006; **72**(4): 503-511.

[15] Hadi MNS. **Comparative Study of Eccentrically Loaded FRP Wrapped Columns**. *Composite Structures* 2006; **74**(2): 127-135.

[16] Hadi MNS, Widiarsa IBR. **Axial and Flexural Performance of Square RC Columns Wrapped with CFRP under Eccentric Loading**. *Journal of Composites for Construction* 2012; **16**(6): 640-649.

[17] Bisby L, Ranger M. **Axial–Flexural Interaction in Circular FRP-Confined Reinforced Concrete Columns**. *Construction and Building Materials* 2010; **24**(9): 1672-1681.

[18] Hassan W, Hodhod O, Hilal M, Bahnasaway H. **Tests on FRP-Retrofitted Tension-Controlled Eccentric and Biaxial High Strength Concrete Columns**. *Composite Structures* 2021; **276**: 114536.

[19] Punurai W, Hsu C-TT, Punurai S, Chen J. **Biaxially Loaded RC Slender Columns Strengthened by CFRP Composite Fabrics**. *Engineering Structures* 2013; **46**: 311-321.

[20] Harries KA, Carey SA. **Shape and "Gap" Effects on the Behavior of Variably Confined Concrete**. *Cement and Concrete Research* 2003; **33**(6): 881-890.

[21] Wang L-M, Wu Y-F. **Effect of Corner Radius on the Performance of CFRP-Confined Square Concrete Columns: Test**. *Engineering Structures* 2008; **30**(2): 493-505.

[22] Hadi MNS, Pham TM, Lei X. **New Method of Strengthening Reinforced Concrete Square Columns by Circularizing and Wrapping with Fiber-Reinforced Polymer or Steel Straps**. *Journal of Composites for Construction* 2012; **17**(2): 229-238.

[23] Moran DA, Pantelides CP. **Elliptical and Circular FRP-Confined Concrete Sections: A Mohr–Coulomb Analytical Model**. *International Journal of Solids and Structures* 2012; **49**(6): 881-898.

[24] Pham TM, Doan LV, Hadi MNS. **Strengthening Square Reinforced Concrete Columns by Circularisation and FRP Confinement**. *Construction and Building Materials* 2013; **49**: 490-499.

[25] Priestley MJN, Seible F. **Design of Seismic Retrofit Measures for Concrete and Masonry Structures**. *Construction and Building Materials* 1995; **9**(6): 365-377.

[26] Yan Z, Pantelides CP. **Fiber-Reinforced Polymer Jacketed and Shape-Modified Compression Members: II - Model**. *ACI Structural Journal* 2006; **103**(6): 894-903.

[27] Yan Z, Pantelides CP. **Concrete Column Shape Modification with FRP Shells and Expansive Cement Concrete**. *Construction and Building Materials* 2011; **25**(1): 396-405.

[28] Si Youcef Y, Amziane S, Chemrouk M. **Geometrical Effect on the Behavior of CFRP Confined and Unconfined Concrete Columns**. *Journal of Reinforced Plastics and Composites* 2010; **29**(17): 2621-2635.

[29] Li G, Maricherla D, Singh K, Pang S-S, John M. **Effect of Fiber Orientation on the Structural Behavior of FRP Wrapped Concrete Cylinders**. *Composite Structures* 2006; **74**(4): 475-483.

[30] Lam L, Teng J. **Strength Models for Fiber-Reinforced Plastic-Confined Concrete**. *Journal of Structural Engineering* 2002; **128**(5): 612-623.

[31] Lam L, Teng JG. **Design-Oriented Stress-Strain Model for FRP-Confined Concrete in Rectangular Columns**. *Journal of Reinforced Plastics and Composites* 2003; **22**(13): 1149-1186.

[32] ACI Committee 318. **Building Code Requirements for Structural Concrete and Commentary ACI 318M-11**. American Concrete Institute; 2011.

[33] Popovics S. **A Numerical Approach to the Complete Stress-Strain Curve of Concrete**. *Cement and Concrete Research* 1973; **3**(5): 583-599.

[34] Tasdemir M, Tasdemir C, Akyüz S, Jefferson A, Lydon F, Barr B. **Evaluation of Strains at Peak Stresses in Concrete: A Three-Phase Composite Model Approach**. *Cement and Concrete Composites* 1998; **20**(4): 301-318.

[35] ASTM D7565. **Standard Test Method for Determining Tensile Properties of Fiber Reinforced Polymer Matrix Composites Used for Strengthening of Civil Structures**. ASTM International; 2010.

[36] Li J, Hadi MNS. **Behaviour of Externally Confined High-Strength Concrete Columns under Eccentric Loading**. *Composite Structures* 2003; **62**(2): 145-153.